Influence of alloying elements on the thermal contraction of peritectic steels during initial solidification

C. Bernhard*[1] and G. Xia[2]

A modified SSCT (submerged split chill tensile) test was used to measure the contraction forces occurring during the solidification of steels with a carbon content of between 0·05 and 0·2 wt-% at constant Mn (1·55%) and Si (0·3%) contents. Further test series were performed with varying Si, V, Cr, Mn, Ni and Nb contents at a constant C content of 0·1%. Any cracks generated were detected, counted and measured. The total crack length allows conclusions to be drawn about the influence of alloying elements on crack susceptibility. The measured results match very well with results calculated from hot tearing criteria. Besides the steel composition, the superheat of the melt proved to be the most important factor in crack formation caused by contraction.

Keywords: Peritectic steels, Solidification, Thermal contraction, Alloying effects

Introduction

The thermal contraction of the solidifying shell in the meniscus region of a continuous casting mould is highly important for the surface and subsurface quality of the cast product. It is well known that peritectic steels with an equivalent carbon content of between 0·1 and 0·12 wt-% show the highest contraction of all carbon steels.[1] This is often related to the relatively small range of δ–γ transformation during and immediately after solidification. Peritectic steel grades are therefore crack sensitive and more difficult to cast than others. Wolf has published a comprehensive survey of this topic.[2]

The current paper presents the results of a joint research project between Voestalpine Stahl and the Department of Metallurgy at the University of Leoben. An apparatus for the *in situ* measurement of tensile forces was adopted for the measurement of contraction induced forces during initial solidification. This method gives a quantitative indication of the influence of alloying elements on thermal contraction and crack susceptibility during initial solidification. The cooling conditions were adjusted to those of a slab casting mould.

For a standard steel grade with 1·55 wt-%Mn and 0·3 wt-%Si, the carbon content was varied between 0·05 and 0·2 wt-%. In another test series the Mn content was varied between 0 and 1·55 wt-%, the Si content from 0 to 0·3 wt-%, Cr from 0 to 0·2 wt-%, Ni from 0 to 0·3 wt-%, Nb from 0 to 0·05 wt-% and V from 0 to 0·06 wt-%.

Every steel grade shows an individual pattern in the development of contraction forces during solidification. This behaviour can be correlated with the onset of phase transformation in the solid state. The contraction curves measured are a promising and unique basis for future numerical simulation work on shrinkage in the mould.

Method

In order to measure the contraction force during solidification, a test method is used that has been slightly modified from that previously used in hot tensile tests (e.g. Refs. 3–5). A split chill test body is submerged in the liquid steel inside an induction furnace (Fig. 1). The surface of the test body is spray coated with a thin zirconium oxide layer in order to control heat flux and to minimise friction forces. A steel shell solidifies around the test body, with the main crystallographic orientation perpendicular to the interface, similar to the situation in a continuous casting mould. The upper part of the test body is fixed, whereas the position of the lower part is controlled via a servo-hydraulic system. This allows both movement of the part with controlled velocity, and holding in a fixed position against increasing contraction forces. The second procedure allows the investigation of the influence of steel composition and cooling rate on thermal contraction forces and crack formation.

The test series reported here were performed on the steel grade X65, which has a nominal composition of 0·1 wt-%C, 1·55 wt-%Mn and 0·3 wt-%Si. Table 1 gives an overview of the variations in the alloying elements considered.

The temperature inside the test body is measured by two thermocouples positioned at a defined distance from the surface. Measuring the temperature increase allows the heat flux at the test body/steel shell interface to be calculated. Heat flux is appropriately adjusted to the process being simulated by means of a spray coated zirconium oxide layer. A thickness of $0{\cdot}4 \pm 0{\cdot}02$ mm

[1]Christian Doppler-Laboratory for Metallurgical Fundamentals of Continuous Casting, University of Leoben, Austria
[2]Voestalpine STAHL GmbH, Austria

*Corresponding author, email Christian.Bernhard@mu-leoben.au

Published by Maney on behalf of the Institute
Received 29 April 2005; accepted 31 August 2005
DOI 10.1179/174328106X94717

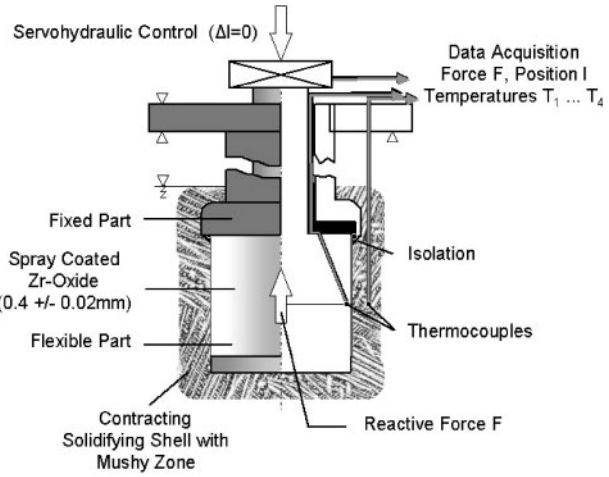

1 Test method, schematic[3–5]

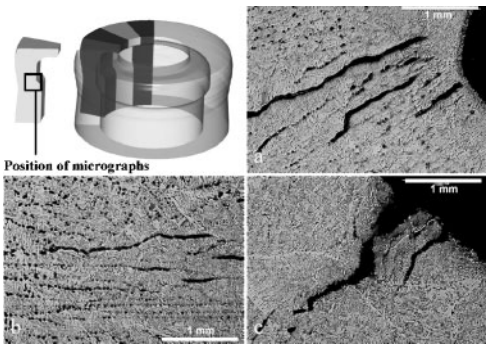

a open internal cracks; *b* segregated internal cracks; *c* surface cracks. Etching: Bêchet–Beaujard

2 Preparation of the metallographic specimen and micrographs of typical cracks types

allows a reduction in the integral heat flux (IHF) to a mean value of $1{\cdot}21 \pm 0{\cdot}08$ MW m^{-2}.

During solidification, the reaction force of the lower part of the test body on the thermal contraction of the steel shell is measured by a load cell. After 25 s of solidification, the test body emerges from the melt. The reaction force in the axial direction reduces to 0, the ongoing contraction leads to shrinkage stresses in the radial direction only. After cooling to room temperature, the solidified shell is separated from the test body. Sixteen metallographic specimens with a height of 30 mm each are cut from the circumference of the shell, polished and etched as shown in Fig. 2. The specimens are subjected to metallographic examination in which the cracks that divided into three groups (segregated internal cracks, open internal crack, surface cracks) are counted and their length is measured. Figure 2 shows also micrographs of the characteristic crack types. The total crack length (TCL) is an indicator of the crack susceptibility. Notice that in the case of a contraction test specimen, surface cracks are most frequently caused by the propagation of internal cracks to the surface and must therefore not be mistaken for any of the several types of surface cracks which occur in continuous casting, forming in the brittle temperature range II (BTR II). Within the scope of the current project, all observed cracks are considered as actuated by contraction, allowing TCL to be defined as a characteristic value for contraction induced crack formation.

Results and discussion

Figure 3 gives an example of the reaction force over time for a 0·05 wt-%C steel together with the calculated shell growth (f_s=solid fraction). The dotted lines symbolise the onset and end of δ–γ transformation, and the black points indicate the measured shell thickness and its standard deviation. As can be seen, thermal contraction starts a few seconds after solidification and reaches a maximum after 17 s. The subsequent decrease in force may either be a consequence of partial defect formation in the shell or a result of creep. As will be shown in detail below, the metallographic examination indicates only a relatively small number of cracks. Creep should therefore be responsible for shell weakening in the 0·05 wt-%C steel grade. The maximum reaction force during testing will be used below as a characteristic value for the comparison of shrinkage in the different steel grades.

For other steel grades, e.g. the 0·128 wt-%C steel, the contraction force increases relatively quickly and reaches a plateau at a more or less constant force, Fig. 4. This is typical for all the steels tested with a carbon content between 0·1 and 0·13 wt-%, and is a result of the onset of δ–γ transformation immediately during solidification.

The steels with 0·2 wt-%C show a different behaviour again. The curves seem to be similar to those of the 0·05 wt-%C steels: after reaching a relatively low maximum, the force decreases. However, in contrast to the 0·05 wt-%C steels, partial crack formation is the main reason for shell weakening, as will be discussed below.

The different phase transformation sequences in hyper- and hypoperitectic steels therefore result not

Table 1 Composition of the steel grades tested (in wt-%)

	C	Si	V	Cr	Mn	Ni	Nb
A	0·05–0·2	0·3	–	–	1·55	–	–
B	0·1	0·02–0·3	–	–	1·55	–	–
C	0·1	0·3	–	–	0·15–1·55	–	–
D	0·1	0·3	–	0·2	1·55	–	–
E	0·1	0·3	–	–	1·55	0·3	–
F	0·1	0·3	0·06	–	1·55	–	–
G	0·1	0·3	–	–	1·55	–	0·03–0·05

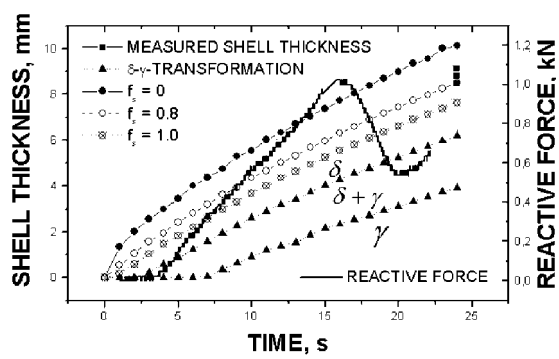

3 Reactive force *v.* time for a 0·05 wt-% carbon steel, with isotherms for solid fractions of 0, 0·8 and 1 and isotherms for the δ–γ transformation

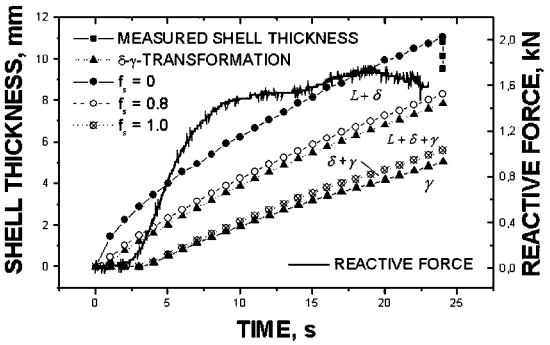

4 Reactive force *v.* time for a 0·128 wt-% carbon steel, with isotherms for solid fractions of 0, 0·8 and 1 and isotherms for the δ–γ transformation

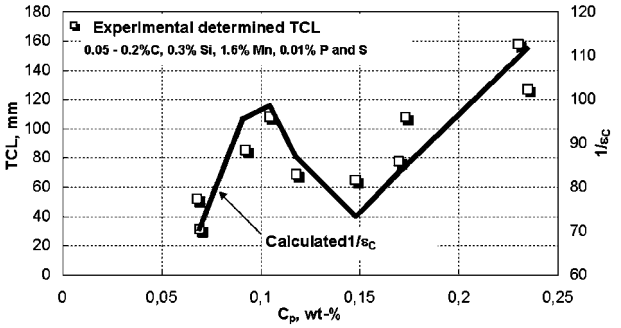

6 Total crack length and calculated $1/\varepsilon_c$ *v.* equivalent carbon content c_p, from Ref. 7

only in different maximum contraction forces but also in a different development of contraction during initial solidification. Steels with between 0·1 and 0·13 wt-%C reach the maximum contraction force within a few seconds of solidification. This is, as documented in a number of papers (summarised in Ref. 2), the reason for the formation of surface depressions. The results also give an indication of the difficulties in adjusting the mould taper to the shrinkage of different steel grades.

A careful interpretation of the results demands the use of an equivalent carbon content, to summarise the influence of all alloying elements on the peritectic reaction[6]

$$c_p = [\%C] + 0{\cdot}04[\%Mn] + 0{\cdot}1[\%Ni] - 0{\cdot}14[\%Si] \qquad (1)$$

Figure 5 shows the maximum reaction force measured versus the equivalent carbon content for series A. Whereas steels with a low carbon content (0·05 wt-%) and a higher c_p (0·2 wt-%) show relatively small shrinkage forces, the contraction force of steels with between 0·08 and 0·15 wt-%c_p is high.

The TCL behaves to some extent in a similar way. Figure 6 shows the results of test series A with a carbon content between 0·05 and 0·2 wt-%. In addition, a calculated curve for $1/\varepsilon_c$ is plotted as a quantitative indication of the hot tearing susceptibility. The calculation procedure for ε_c, the critical strain of crack formation, is described below. The close connection between the TCL and equivalent carbon content is apparent. The low carbon steel grades (0·05 wt-%) are relatively crack insensitive, pointing at the onset of creep at an early stage of contraction, therefore preventing the formation of hot tears. Around 0·1 wt-%c_p, both the contraction force and the measured TCL show a maximum. Between 0·12 and 0·15 wt-%c_p, TCL decreases, and rises again above 0·17 wt-%c_p. The results for the test at less than 0·15 wt-%c_p lead to the assumption that higher contraction forces result in a higher number and length of cracks. As an exception, the steels with a c_p of around 0·2 wt-% reveal a low maximum contraction force, leading to an extremely high TCL, e.g. three times higher than for the 0·05 wt-%C steels. Apparently, the crack initiation and propagation starts at low contraction forces and weakens the supporting cross section of the shell. This confirms previous results from tensile tests with the same apparatus on 0·2 wt-%C steels,[3] indicating a particularly low critical strain.

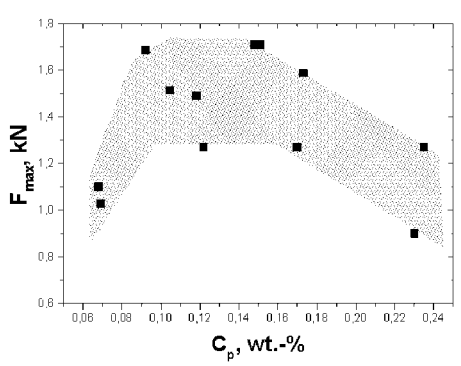

5 Maximum reactive force *v.* equivalent carbon content c_p

Recently, Pierer and Bernhard[7] applied two common hot tearing criteria to the results of the above described test series. Figure 6 shows a plot of the calculated quantitative hot tearing susceptibility using the reciprocal value of the critical strain ε_c. The critical strain of crack formation ε_c was calculated using the following equation, proposed by Won *et al.*[8]

$$\varepsilon_c = \frac{\varphi}{\Delta T_B^n \cdot \dot{\varepsilon}^m} \qquad (2)$$

The parameters in equation (2) are the BTR ΔT_B and the strain rate $\dot{\varepsilon}$. φ is a constant and m and n are the strain rate sensitivity and the BTR exponent respectively. ΔT_B is defined as the temperature range between LIT (liquid impenetrable temperature) and ZDT (zero ductility temperature), where LIT and ZDT correspond to the isotherm for solid fractions of 0·9 and 0·99 respectively, as proposed by Clyne *et al.*[9] Therefore, ΔT_B can be calculated using microsegregation analysis. Figure 7*a* shows the values of ΔT_B calculated using the solidification software IDS[10] in addition to the TCL. Calculation of the strain rate was carried out using the relative contraction β between ZDT and Z50 (Z50 is the temperature at about 50 K below solidus). Figure 7*b* shows the relative contraction β over the equivalent carbon content, also calculated using IDS. With the relationship $\dot{\varepsilon} = \beta/t$ and assuming a constant cooling rate $\dot{T}$ of about 1 K s^{-1} the strain rate can be expressed as follows ($t = ZDT - Z50)/\dot{T}$)

$$\dot{\varepsilon} = \frac{\beta}{ZDT - Z50} \qquad (3)$$

Finally, the critical strain of crack formation (equation 2) can be calculated with the values of ΔT_B and $\dot{\varepsilon}$ determined as described above, and the proposed

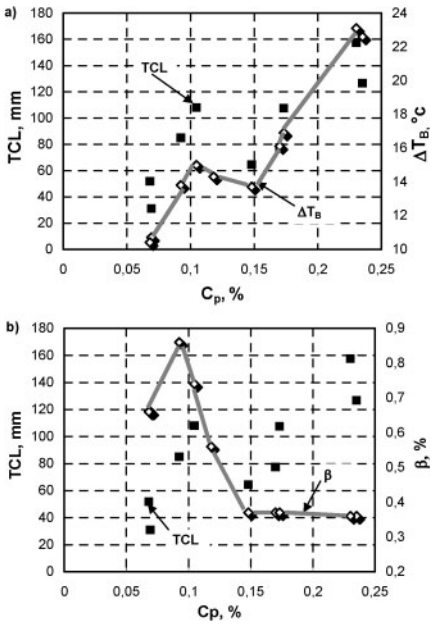

7 Brittle temperature range ΔT_B, relative contraction β and TCL *v.* equivalent carbon content (from Ref. 7)

parameters of φ, n and m.[8] The reciprocal value of ε_c, which is plotted in Fig. 6, was finally used as a quantitative description of the hot tearing susceptibility over the equivalent carbon content.

The results confirm the tendency of the measured TCL: for c_p=0·1, both the critical temperature range and the contraction within the critical temperature range (increasing $\dot{\varepsilon}$) show a maximum. This causes a minimal critical strain and a maximum crack susceptibility. If c_p exceeds 0·15 wt-%, the increase in ΔT_B becomes responsible for the decrease in critical strain. These considerations provide a feasible explanation of the results of series A.

Test series B–G were performed with the standard steel composition (0·1 wt-%C, varying Mn and Si contents, 1·55 wt-%Mn, 0·3 wt-%Si, 0·12 wt-%c_p for all other tests) and varying Si, Mn, Cr, Ni, Nb and V contents (Table 1). The results can be summarised as follows:

(i) at a very low Si content the crack length increases and the contraction force remains constant

(ii) Mn behaves neutrally, neither crack susceptibility nor the contraction force are significantly influenced

(iii) both Cr and Ni have a negative influence on crack sensitivity: an increase in Cr content to 0·2 wt-% increases the TCL from 70 to 85−95 mm. For 0·3 wt-%Ni the crack length amounts to 100−110 mm. Both elements lower the contraction force slightly

(iv) an increase in Nb content to 0·03 wt-% worsens crack susceptibility, whereas a further increase to 0·05 wt-% lowers the TCL. This behaviour might be explained by the onset of interdendritic (Ti,Nb) (C,N) precipitation at higher temperature

(v) V behaves neutrally, neither crack length nor the contraction force is significantly influenced.

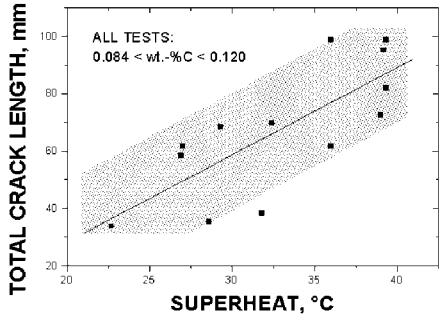

8 Total crack length *v.* superheat for tested steels with carbon between 0·084 and 0·12 wt-% (1·55 wt-%Mn, 0·3 wt-%Si)

Another important testing parameter is the superheat of the melt. The temperature of the melt is adjusted to between 25 and 35 K above the liquidus before testing, but the online temperature measurements during testing often yield more scattered values resulting from temperature gradients inside the melt. For the current test series, the fluctuations range between 20 and 40 K. The variation in superheat allows a correlation with the TCL. As can be seen in Fig. 8, an increase in the superheat has a detrimental influence on crack susceptibility. Besides the variation in steel composition, superheat seems to be the most important factor. An increase in superheat by 10°C nearly doubles the TCL. Conclusions for the role of superheat in continuous casting must be drawn carefully, although the results correspond with plant observations.

Summary

In this paper, the thermal contraction during solidification of peritectic steels was measured. The test method gives a qualitative indication of the influence of alloying elements on thermal contraction and contraction induced crack formation, such as the formation of longitudinal cracks. Some of the results were anticipated from the literature. Others, such as the influence of carbon on the development of the contraction force during initial solidification, offer new perspectives and confirm plant observations.

Steels with an equivalent carbon content of 0·1 and more than 0·17 wt-%C are more crack sensitive than low carbon steels. Steels with 0·1 and 0·15 wt-%C tend to higher contraction forces. The contraction force builds immediately upon initial solidification. This is the reason for the formation of surface depressions, as well as the higher sensitivity to the formation of longitudinal surface cracks.

The tests series with varying content of other elements indicate that Mn and V behave relatively neutrally, whereas Cr and Ni worsen the crack sensitivity. Within the concentration range investigated, Si improves the crack susceptibility.

A variation in superheat can significantly influence the crack susceptibility. An increase in superheat by 10°C nearly doubles crack formation. This again corresponds with plant observations.

In future work, further results of contraction tests and tensile tests with the SSCT (submerged split chill tensile) apparatus will provide the opportunity to fit crack

criteria. A comprehensive quantification of the influence of alloying elements on contraction induced crack formation will assist in the further improvement of quality control systems.

Acknowledgement

An updated version of a presentation at the 4th European Continuous Casting Conference organised by IoM Communications in Birmingham, UK in October 2002.

References

1. A. Jablonka, K. Harste and K. Schwerdtfeger: *Steel Res.*, 1991, **62**, 24–33.
2. M. Wolf: in 'Continuous casting 9'; 1997, Warrendale, PA, Iron and Steel Society.
3. C. Bernhard, H. Hiebler and M. Wolf: *Ironmaking Steelmaking*, 2000, **27**, 450–454.
4. C. Bernhard, W. Schützenhöfer, H. Hiebler and M. Wolf: Proc. 2nd Int. Conf. on 'Science and technology of steelmaking', April 2001, Swansea, UK, 87.
5. C. Bernhard, H. Hiebler and M. Wolf: *Rev. Metall., Cah. dInf. Tech.*, 2000, **97**, 333–344.
6. A. A. Howe: 'Segregation and phase distribution during solidification of carbon, alloy and stainless steels', EUR 13303; 1991, Luxembourg, ECSC.
7. R. Pierer and C. Bernhard: *Berg Hütt. Monatsh.*, 2004, **149**, 95–101.
8. Y. M. Won, T.-J. Yeo, D. J. Seol and K. H. Oh: *Metall. Mater. Trans. B*, 2000, **31B**, 779–794.
9. T. W. Clyne, M. Wolf and W. Kurz: *Metall. Mater. Trans. B*, 1982, **13B**, 259–266.
10. J. Miettinen: *Metall. Mater. Trans. B*, 1997, **28B**, 281–297.